

FakeCatcher: Detection of Synthetic Portrait Videos using Biological Signals

Umur Aybars Ciftci
Binghamton University
uciftci@binghamton.edu

Ilke Demir
Facebook
idemir@fb.com

Abstract

As we enter into the AI era, the proliferation of deep learning approaches, especially generative models, passed beyond research communities as it is being utilized for both good and bad intentions of the society. While generative models get stronger by creating more representative replicas, this strength begins to pose a threat on information integrity. We would like to present an approach to detect synthesized content in the domain of portrait videos, as a preventive solution for this threat. In other words, we would like to build a deep fake detector. Our approach exploits biological signals extracted from facial areas based on the observation that these signals are not well-preserved spatially and temporally in synthetic content. First, we exhibit several unary and binary signal transformations for the pairwise separation problem, achieving 99.39% accuracy to detect fake portrait videos. Second, we use those findings to formulate a generalized classifier of authentic and fake content, by analyzing the characteristics of proposed signal transformations and their corresponding feature sets. We evaluated FakeCatcher both on Face Forensics dataset [46] and on our newly introduced Deep Fakes dataset, performing with 82.55% and 77.33% respectively. Third, we are also releasing this mixed dataset of synthesized videos that we collected as a part of our evaluation process, containing fake portrait videos "in the wild", independent of a specific generative model, independent of the video compression, and independent of the context. We also analyzed the effects of different facial regions, video segment durations, and dimensionality reduction techniques and compared our detection rate to recent approaches.

1. Introduction

The technological advancements in deep learning have started to revolutionize our perspective about how we solve many difficult problems in computer vision, robotics, and related areas. Common deep learning models for recognition, classification, and segmentation tasks tend to improve how we and machines perceive, learn, and analyze

the world. On the other hand, the developments in generative models significantly increased how we and machines tend to mimic the world and create realistic data. Even though it is easy to speculate dystopian scenarios based on both analysis and synthesis approaches, the latter brought the immediate threat on information integrity by disabling our biological "detectors" of authentic content: we cannot simply look at an image to understand if it is fake or not.

Following the recent initiatives for democratization of AI, generative models [22, 45, 62, 56] are getting more popular and reachable. Although the widespread use of GANs is positively impacting some technologies (i.e., personalized avatars [40], animations [44], and image inpainting [37]), there are also uses of GANs with malicious intent, which impacts the society by introducing inauthentic content (i.e., celebrity porn [3], fake news [2], and AI art [1]). This lack of authenticity and increasing information obfuscation pose real threats to individuals, criminal system, and information integrity. As every technology is built simultaneously with the counter-technology to neutralize its negative effects, we believe that it is the perfect time to develop a deep fake detector to prevent this threat before having serious consequences.

We observed that, although GANs are powerful enough to learn and generate photorealistic visual and geometric signals beyond the discriminative capabilities of human eyes, biological signals hidden by nature are still not easily replicable. Biological signals are also intuitive and complementary ingredients of facial videos, for which generative models are mostly applied in order to create deep fakes. Moreover, videos contain another layer of complexity for the synthesized content to satisfy the consistency in the time dimension, in addition to the signals' spatial coherence. To complete this narrative, our approach exploits hidden biological signals (such as heart rate) to detect inauthentic content on portrait videos, independent of the source of creation and transmission.

Our main contributions include,

- formulations of signal transformations to exploit spatial coherence and temporal consistency of biological signals for pairwise separation task,

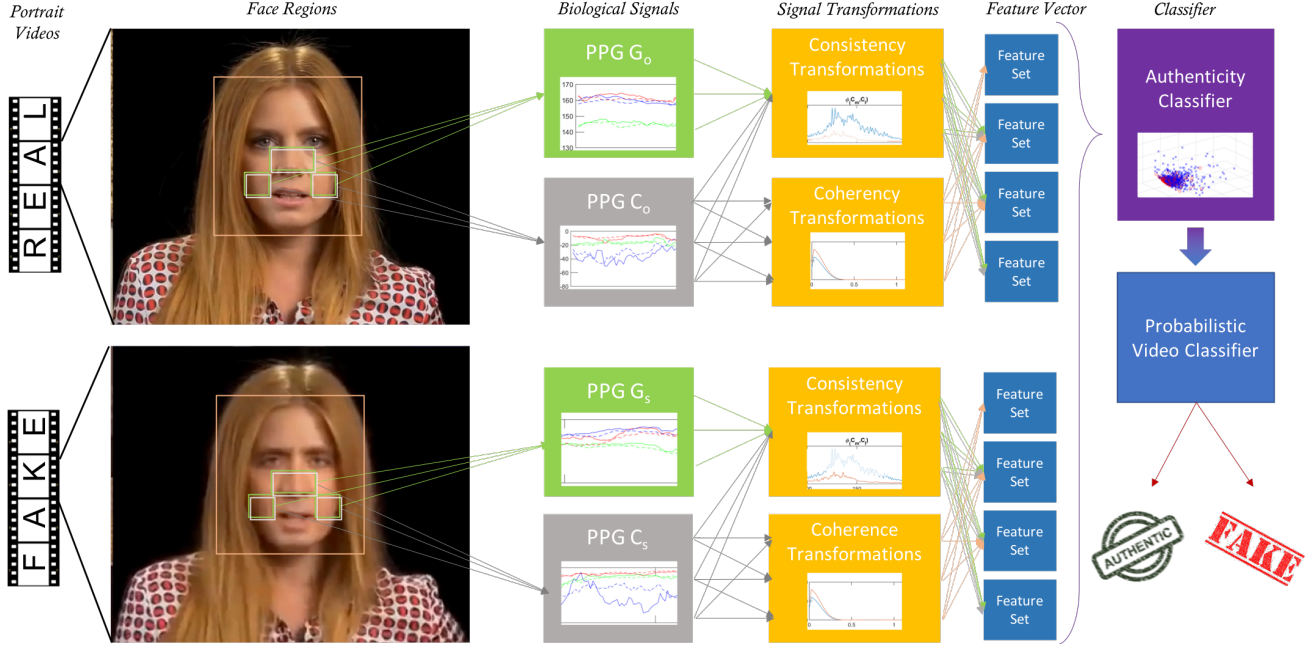


Figure 1. **System Overview:** We extract biological signals from three facial regions on authentic and fake portrait video pairs. We apply several transformations to compute the spatial coherence and temporal consistency, capture the signal characteristics in feature sets, and train a binary probabilistic SVM. Then we aggregate authenticity probabilities of all segments to decide whether the video is a deep fake.

- a generalized synthetic portrait video detector which can catch "deep fake"s based on biological signals,
- experimental validation of exploitability of spatial coherence and temporal consistency of biological signals for authenticity classification,
- a diverse and unconstrained dataset of synthesized portrait videos to create a test bed for inauthentic content detection in the wild.

Our system processes input videos by collecting video segments with facial parts, defining several regions of interests (ROIs), and extracting several biological signals from those regions. In the first part, those signals, their transformations to different domains (time, frequency, time-frequency), and their correlations in different domains are examined to formulate a solution to pairwise separation. In the second part, we combine the discoveries from the pairwise context with feature extractors in the literature to come up with a generalized authenticity classifier working in a high dimensional feature space. We also aggregate the class probabilities of segments into a binary decision of "fake or authentic" for the video. The system is depicted in Figure 1.

To evaluate FakeCatcher, we collected over 100 videos, totaling up to 59 GB, from the internet. It is important to note that, unlike existing datasets, our Deep Fakes dataset includes "in the wild" videos, independent of the generative model, independent of the resolution, independent of

the compression, and independent of the content and context. We detect the in authentic content on our dataset with 77.33% accuracy. We also tested our approach on Face Forensics dataset [46], which reaches 82.55% accuracy to classify inauthentic content. We analyzed the effects of segment durations, facial regions, and dimensionality reduction techniques on those datasets, on our feature sets, and on our signal transformations.

2. Related Work

Traditionally, image spoofing and forgeries have been an important topic in forensics and security, with corresponding pixel and frequency analysis solutions to detect visual artifacts. These methods, in addition to early deep learning based generative models, were able to create some inauthentic content, however the results were easily classified as fake or real by human eyes. As the generative models become stronger and easier to reach, develop, and train, the amount of inauthentic content began to spread widely. This disinformation creates dystopian scenarios related to frauds, fake news, counterfeit authentication, miscarriage of justice, and security risks.

2.1. GAN Empowerment

Following the Generative Adversarial Networks proposed by Goodfellow et al. [22], deep learning models have been advancing for generative tasks for inpainting [27],

translation [62], and editing [11]. GAN architecture can be simplified as the "game" between the generator network and the discriminator network. Generator adapts its parameters to create realistic images that mimic the distribution of the real data, and discriminator adapts its parameters to correctly differentiate real and fake images created by the generator. Inherently, all generative approaches suffer from the control over generation. In the context of GANs, this problem is mostly explored by Variational Autoencoders (VAE) and Conditional GANs to control the generation by putting constraints in the latent space [32, 52]. In addition to improving the control over GANs, other approaches improved the training efficiency, accuracy, and realism of GANs by deep convolutions [45], Wasserstein distances [23], least square [38], and progressive growing [30]. All these advancements in the generative power, realism, and efficiency of GANs resulted in the development of "deep fake"s.

2.2. Synthetic Faces

Since Viola-Jones [55], computer vision community treasures the domain of facial images and videos as one of the primary application domains. Following the pattern, applications and explorations of GANs have been done for face completion [37], facial attribute manipulation [49, 16, 24], frontal view synthesis [26], facial reenactment [31, 53, 59], identity-preserving synthesis [8] and expression editing [19]. In particular, VAEs and GANs for facial reenactment and video synthesis resulted in the emergence of "deep fake" concept, which can be expressed as replacing the face of a target person with another face in a given video. Although the exact approach is not published, the mainstream deep fake generator is assumed to consist of two autoencoders trained on source and target videos, while keeping the encoder weights similar, so that same general features (illumination, motion, expression, etc.) can be embedded in the encoder and face-specific features can be integrated by the decoder. Another approach, Face2Face [53], reconstructs a target face from a training video and then warps it with the blend shapes obtained by the source video in real-time. Deep Video Portraits [31] and vid2vid [56] follow this approach and employ GANs instead of blend shapes. Although the results of all of these approaches can be very realistic, there are still skipped frames and face misalignments due to illumination changes, occlusions, video compressions, and sudden motions. Such imperfections are best caught by biological signals that we will propose in the next section.

2.3. Image Forensics

In par with the increasing number of inauthentic facial images and videos, methods for detecting authenticity of such content have also been proposed. Those are mostly based on finding inconsistencies in images, such as detect-

ing distortions [10], finding compression artifacts [9], and assessing image quality [21]. However, for synthetic images in our context, the noise and distortions are harder to detect due to the non-linearity and complexity of the learning process [34]. It is possible to investigate the color and noise distributions of specific networks [35, 48], or training CNNs for synthetic images [4, 51], but catching synthetic images and videos in the wild is still an open research topic. The last approach we would like to introduce in this domain, which can be considered as the most similar to ours as the only fake detector on videos, exploits blinks to detect inauthentic facial videos [36] as another biological signal.

3. Biological Signals

The remote extraction of biological signals roots back to the medical communities to reduce the intrusion on the patients for specific measurements, such as heart rate. Observing subtle color and motion based signals from videos [58, 15] enabled methodologies like remote photoplethysmography (rPPG or iPPG) [47, 43] and head motion based ballistocardiogram (BCD) [7] for non-intrusive heart rate detection from facial RGB videos. We will mostly focus on PPG as it is more robust against dynamic scenes, while BCD needs static videos. Several approaches proposed improvements to PPG, using chrominance features [18], G channel components [61], optical properties [20], kalman filters [5], and different facial areas for signal extraction [61, 54, 20, 47].

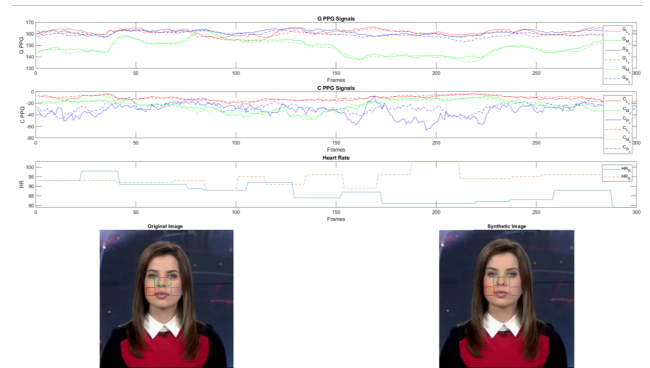


Figure 2. **Biological Signals:** Green and chrom-PPG signals from left (L), middle (M), and right (R) face regions, heart rates and sample frames of an original-synthetic video pair of 10 seconds.

We believe all of these PPG variations contain valuable information in the context of inauthentic videos. In addition, their inter-consistency for real video segments are higher than those from fake videos. Multiple signals also help us regularize the environmental effects (illumination, occlusion, motion, etc.) for robustness. Thus we will work on the following six signals that are combinations of G channel-based [61] (robust against compression artifacts)

and chrominance-based PPG [18] (robust against illumination artifacts) on left cheek, right cheek [20], and mid-region [54], namely $\{G_L, G_R, G_M, C_L, C_R, C_M\}$. Figure 2 demonstrates those signals extracted from an authentic and a synthetic video segment.

4. Characteristics of Biological Signals on Original-Synthetic Video Pairs

In order to understand the nature of biological signals in the context of synthetic content, we first compared signal responses on original and synthetic video pairs using traditional signal analysis methods as shown in Figure 4. The motivation behind this analysis is to find the best error metric between pairs of original and synthetic facial videos with similar content. Concluding on an error metric directs us for which signals and which features to use for a generalized classifier. This analysis also gives ground for understanding generative systems in terms of biological replicability.

4.1. Statistical Features

Setting a sample toy subset (150 pairs of videos in the test set of Face Forensics [46]), we cut each video into ω frame windows (the effect of ω is extensively analyzed in Section 6.2). Our analysis starts by comparing simple metrics as the mean, standard deviation, and min-max ranges of PPG signals from original and synthetic video pairs, achieving the best accuracy as 65%. Next, we investigated same metrics on absolute values of differences between consecutive frames in original and synthetic videos, achieving the best accuracy of 75.69%. Since it was obvious that these features are aggregating the whole segment signals into single numbers which are not representative enough, we wanted to pursue metrics in other domains.

4.2. Power Spectra

We continued by looking at the power spectrum density (PSD) of those signals S_o and S_s , in linear and in log scale, achieving a best accuracy of 79.33% by $\mu_{P(G_{L_o})} + \sigma_{P(G_{L_o})} - \mu_{P(G_{L_s})} - \sigma_{P(G_{L_s})}$. Fourth, we analyzed discrete cosine transforms (DCT) of the log scale of these signals, with the analysis of including (I, II, III, and IV) variants (see Appendix B) obtaining an accuracy of 77.41%. However this gave us more inspiration about the next comparison: The zero-frequency (DC value) of DCT led us to a significant improvement to 91.33% accuracy. We ran the same evaluation, reaching 84.89% accuracy on the entire Face Forensics dataset and reaching 64.35% accuracy on our Deep Fakes dataset.

4.3. Spatio-temporal Coherence of Multiple Signals

We also ran some analysis to accompany for the coherence of biological signals within each frame. For robustness

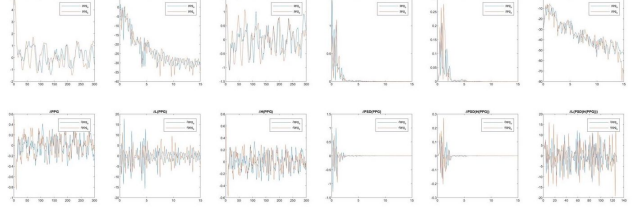


Figure 3. **Original and Synthetic Signal Pairs:** Top row demonstrates several characteristics on the raw signals, bottom row demonstrates the same analysis on the derivative of the signals.

against illumination changes, we alternated to use C_L and C_M , and we computed their cross-correlation of their PSD as $\phi_{P(C_M)P(C_L)}$. On original and synthetic segments, comparing the maximum values gave us 94.57% and mean values gave us 97.28% accuracy. We improved this result by first computing PSDs in the log scale (98.79%) and finally computing the cross power spectral densities (99.39%). This final metric reached an accuracy of 95.068285% on the entire Face Forensics dataset and 73.684211% on our Deep Fakes dataset.

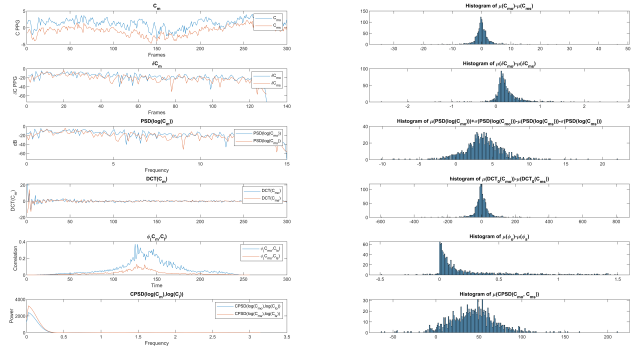


Figure 4. **Pairwise Analysis:** Right: example original-synthetic signal pair, their derivatives δC_M , power spectral densities $PSD(\log(C_M))$, discrete cosine transforms $DCT(C_M)$, cross correlations with C_L , and cross power spectral densities with C_L . Left: Histograms of mean differences of these values for all pairs.

5. Generalized Authentic Content Classifier

Achieving considerably high accuracy for detecting authentic content from pairs of original and synthetic videos, we would like to generalize this approach as a binary classifier for authentic content. In the pair-wise setting, comparison of aggregate features are representative enough. However as these signals are continuous and noisy, we need to extract representative features from the ensemble of those signals to build a generalized classifier. We experimented with several signal transformations in time and frequency domains to explore the artifacts of synthetic videos towards

characteristic features (Table 1).

Symbol	Signal
S	$\{G_L, G_R, G_M, C_L, C_R, C_M\}$
D	$\{ C_L - G_L , C_R - G_R , C_M - G_M \}$
A(S)	autocorrelation
$\hat{A}(S)$	spectral autocorrelation
P(S)	power spectral density
W(S)	Wavelet transform
L(S)	Lyapunov function [39]
G(S)	Gabor-Wigner transform [42]
S_C	$\{C_L, C_R, C_M\}$
D_C	$\{ C_L - C_M , C_L - C_R , C_R - C_M \}$
$A_p(S_C)$	pairwise cross spectral densities

Table 1. **Signal Definitions:** We define the signals and transformation functions that will be used throughout the analysis.

5.1. Feature Sets

Following the signal transformations, we also explored the features to be extracted from those signals. Due to the fact that rPPG is mostly evaluated by the accuracy in heart rate, we researched other features for image authenticity [34], classification of EEG signals [28, 41], statistical analysis [60, 50, 25], and emotion recognition [39, 41]. The feature sets are enumerated in Table 7 together with the reference papers for biological signal classification, we refer the reader to the specific paper for the formulation and detailed explanation of all features.

5.2. Authenticity Classification

With the motivation of being able to detect deep fakes in the wild, we experimented with combinations of transformed biological signals and feature sets to classify all videos into authentic and fake videos. Approaching the problem without any assumptions, but still obtaining interpretable results is the key motivation that lead us to employ SVMs with a RBF kernel [17] for this binary classification task. Appendix A documents our experiments, however we would like to highlight some of them in the main paper, as well as the parameters that affect the classification accuracy. We will denote all experiments with $F_*(T(S))$ where F_* is the feature extractor from Table 7 applied to (transformed) signal $T(S)$ from Table 1. Note that both the signal transformation and the feature extraction can be applied separately to all elements of the inner set.

For our exploration, we randomly split the [46] dataset to training (1540 samples, 60%) and validation sets (1054 samples, 40%). We created feature vectors with maximum and mean (F_1) of cross power spectral densities of C_M and C_L ($A_p(C_M, C_L)$) of all videos in the training set, as it was the feature with the highest accuracy from Section 4.3. Unlike pairwise results, SVM accuracy with $f =$

$F_1(A_p(C_M, C_L))$ was low (68.9394%) but this set a baseline for other methods. Next, we classified by $f = \mu_{P(S)}$ (six features per sample) achieving 68.8805% accuracy, and by $f = \mu_{A_p(D_C)} \cup \mu_{A(S)}$ (9 features per sample) achieving 69.6395% accuracy on the entire [46] dataset.

f	$ f $	\tilde{f}
$F_3(\hat{A}(S))$	4*6	67.5522%
$F_6(L(S))$	600	69.0408%
$F_4(\log(S))$	60	69.0702%
$F_2(S)$	13*6	69.26%
$F_5(P(W(S)))$	390	69.6395%
$F_4(S) \cup F_3(\log(S)) \cup \mu_{A_p(D_C)}$	6*6+4*6+3	71.3472%
$F_4(\log(S) \cup A_p(D_C)) \cup F_1(\log(D_C)) \cup F_3(\log(S) \cup A_p(D_C))$	6*9+6+4*9	72.0114%

Table 2. **Feature Set Experiments:** Signal, applied transformation, and the feature set (left), size of the feature vector (middle), and segment classification accuracy (right) of some experiments.

Some of the experiments that lead us to use a combination of features to improve the accuracy, both on the [46] dataset and our Deep Fakes dataset, are listed in Table 2. Based on the list of experiments (documented in Appendix A), we observed that the "authenticity" (i) can be observed both in time and frequency domains, (ii) is coupled with small motion changes, illumination effects, and compression artifacts in the video thus it is not separable, and (iii) can be discovered from the coherence of multiple biological signals. It is also important to note that the reason that we exhaustively tried all possible feature extractors in the literature is robustness. We would like our system to be independent of any generative model, any compression/transmission artifact, and any content-related influence: a robust and generalized FakeCatcher, based on the essence of consistency and coherence of biological signals in authentic videos. Our observations together with the experimental results concluded on this feature set for our authenticity classification:

$$f = F_1(\log(D_C)) \cup F_3(\log(S) \cup A_p(D_C)) \cup F_4(\log(S) \cup A_p(D_C)) \cup \mu_{\hat{A}(S)} \cup \max(\hat{A}(S))$$

The SVM classifier trained with these features on the [46] dataset resulted in 75% accuracy, and on our Deep Fakes dataset resulted in 77.33% accuracy.

5.3. Probabilistic Video Classification

As mentioned in the beginning of Section 4.1, we divide the videos into some intervals of w frames for authentic-

ity classification. Considering that our end goal is to classify videos, not only segments, we need to aggregate the segment classification into video classification. First, we converted segment classes to video class by majority voting. The segment classification accuracy of 75% increased to 78.1879%, hinting that some hard failure segments can be neglected assuming that they contain significant motion or illumination changes. We computed the true threshold to be 0.447, confirming the assumption. Consequently, we converted our SVM to an SVR to return the probability of containing authentic or synthetic facial actors. Then assigning the authenticity based on the mean of the segment class probabilities increased the video classification to 82.5503%.

6. Results and Analysis

Our system utilizes Matlab for heavy signal processing, Open Face library [6] for face detection, libSVM [14] for the classification experiments, and Wavelab [12] for Wavelet transformation and F_5 feature set. We evaluated our detection accuracy on Face Forensics dataset [46] and our Deep Fakes dataset. We have documented all experiments in Appendix A, effects of normalization, filtering, frequency quantization, and DCT coefficients in Appendix B, and ROI analysis on both DF and FF datasets with five different region options in Appendix C. Below, we will discuss some analysis on segment durations ω , and dimensionality reduction of techniques on the feature set f . We also included a comparison section to establish our system as the first approach analyzing biological signals on inauthentic portrait videos.



Figure 5. **Deep Fakes Dataset:** We introduce a diverse dataset of original (top half) and fake (bottom half) portrait video pairs.

6.1. Datasets

We analyzed our approach on Face Forensics dataset [46] which has (i) original and synthetic pairs of videos with same content and actor, and (ii) a compilation of original and synthetic videos, both of which are created using the same generative model. We also collected 114 fake portrait videos from various sources, totaling up to 37 minutes, and 59 GBs. We trimmed the non-portrait parts of the videos, and coupled them with their original pairs. Figure 5 demonstrates a subset of Deep Fakes dataset, originals in the top half and fakes in the bottom half. The aspect ratio, size, frame rate ([25, 30] fps), resolution, compression, resource, and generative source of the videos significantly varies within the dataset. The dataset is released on our project page¹ for the community.

ω	#segments	dataset	s. accuracy	v. accuracy
64	1886	FF test	95.75%	-
128	871	FF test	96.55%	-
256	387	FF test	98.19%	-
300	332	FF test	99.39%	-
64	7619	FF	93.61%	-
128	5886	FF	94.40%	-
256	1554	FF	94.15%	-
300	1320	FF	95.15%	-
128	487	DF	73.94%	67.50%
150	394	DF	73.40%	69.44%
180	326	DF	77.33%	75%
240	218	DF	76.36%	70%
300	158	DF	72.22%	57.89%
128	5886	FF	77.50%	82.55%
150	2959	FF	75.93%	78.18%
180	2294	FF	75.87%	78.85%
256	1525	FF	72.55%	73.82%
300	1296	FF	75.00%	75.16%
450	298	FF	70.78%	71.33%
600	247	FF	68.75%	68.42%

Table 3. **Accuracy per Segment Duration:** We document ω , segment count, and corresponding segment and video accuracies, on toy (FF test), entire (FF) [46], and Deep Fakes (DF) datasets. Rows without video accuracy denotes pairwise evaluations.

6.2. Analysis of Segment Duration

The pairwise decision task differs from the main motivation of FakeCatcher, so we analyzed ω per context. Table 3 documents all results on the both the subset and entire [46] dataset, and Deep Fake dataset. The top half shows the effect of ω on the pairwise comparison. Accordingly, the choice of $\omega = 300$ (10 sec) was long enough to detect strong correlations and not include much content based changes.

¹Link is hidden to satisfy anonymity.

For the generalized classifier, we can be more flexible for hard failure segments, because we can depend on the probabilistic video classifier to accompany for those cases. Thus, selecting a relatively smaller segment duration, $\omega = 180$ (6 sec) helped us increase the video classification accuracy while still keeping it long enough to extract the biological signals. Note that the classifier gets less accurate on Deep Fake video classification by increasing ω , this is due to the fact that some videos are very short to have multiple segments in them, so they are discarded for those segment durations.

6.3. Blind Source Separation

To better understand our features, feature sets, and their relative importance, we computed the Fisher criterion to see if we have any linearly separable features. No significantly high ratio was observed, guiding us towards kernel based SVMs and more source separation trials. We also tried PCA (principal component analysis) and CSP (common spatial patterns) to reduce the dimensionality of our feature spaces. Figure 6 shows 3D distribution of authentic (red) and synthetic (blue) samples by the most significant three components found by PCA and CSP, without clear class boundaries. We also tried to condense the feature vector with our best classification accuracy, however we achieved 71% accuracy after PCA and 65.43% accuracy after CSP.

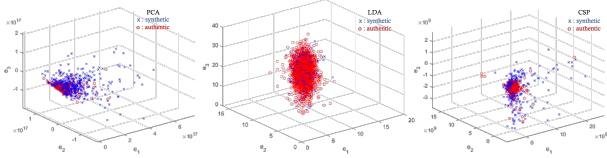


Figure 6. **Source Separation:** We demonstrate authentic (red) and synthetic (blue) samples in the space defined by the three most dominant components, extracted using PCA (left), LDA (mid), and CSP (right).

6.4. Comparison

Even though "deep fake"s are a relatively new problem, there are already a few papers working in this domain. [46] employs another generative model for detection, but their model is restricted to the results of their previous method. [4] also has a high detection rate if the synthetic content is generated by [53] or the VAE network used in the *FakerApp*. [36] also reaches a high accuracy, but they are dependent on eye detection and eye parameterization. All of these approaches employs neural networks blindly and does not make an effort to understand the generative noise that we have experimentally characterized by biological signals. Also it is not clear how they would perform on our Deep Fakes dataset, because it is less constrained and more diverse than their validation data.

6.5. Implementation Details

For each video segment, we apply Butterworth filter [13] with frequency band of $[0.7, 14]$. We quantize the signal using Welch's method [57]. Then we collected the frequencies between $[h_{low}, h_{high}]$ which corresponds to below, in, and high ranges for heart beat. There was no clear frequency interval that accumulated generative noise in biological signals (see Appendix B), so we included all frequencies. In summary, we followed the PPG extraction methods in [61] for G_L, G_M, G_R and [18] for C_L, C_M, C_R . In heart rate extraction, PPG signal goes through significant denoising and componentizing steps to fit the signal into expected ranges and periods. We observed that some signal frequencies and temporal changes that may be considered as noise for heart rate extraction actually contains valuable information for our case. Moreover, as our main motivation is not finding accurate heart rates, we intentionally did not follow some steps of cleaning the PPG signals with the motivation of keeping subtle generative noise.

7. Discussions and Future Work

One approach that stands out from Section 6.4 is to use CNNs for discovering the generative noise from original and synthetic image pairs [4]. Because our component analysis in Section 6.3 do not show strong signs of separability of features, (which is intuitive as generative models and all additive artifacts would contribute to the noisy and non-linear nature of the output), we foresee that an autoencoder can learn the latent representation of biological signal features, later to be used for authenticity classification. However, as the first comprehensive analysis, we wanted to incorporate interpretable features for our classifier, and we see VAEs as the next step of biological feature extractor.

Another future venue we want to explore is to employ our pairwise separation formulation in the loss function of a generative model, to create deeper fakes immune to biological signal analysis. In future, we would like to design a novel generative adversarial loss function to enable creating portrait videos enriched with biological signals, thus even more believable and photorealistic.

8. Conclusion

We present FakeCatcher, an inauthentic portrait video detector based on biological signals. We experimentally validated that spatial coherence and temporal consistency of such signals are not well preserved in GANerated content, thus, we can derive a high dimensional feature vector to aggregate those characteristics for authenticity classification. We evaluated our approach for pairwise separation and for generalized authenticity classification, of video segments and entire videos, on Face Forensics [46] and Deep Fakes datasets, achieving up to 99.39% (pairwise) and 82.55%

Denotation	Explanation	Reference
F_1	mean and maximum of cross spectral density	Section 4.3
F_2	root mean square of differences, standard deviation, mean of absolute differences, ratio of negative differences, zero crossing rate, average prominence of peaks standard deviation of prominence of peaks, average peak width, standard deviation of peak width, maximum derivative, minimum derivative, mean of derivative, mean of spectral centroid	[50]
F_3	count of narrow pulses in the spectral autocorrelation, count of spectral lines in the spectral autocorrelation, average energy of narrow pulses, maximum value of the spectral autocorrelation	[25]
F_4	standard deviation, standard deviation of mean values of 1 second windows, root mean square of 1 second differences, mean standard deviation of differences, standard deviation of differences, mean of autocorrelation, Shannon entropy	[29]
F_5	First n Wavelet coefficients	[28, 39]
F_6	Largest n Lyapunov exponents	[39]
F_7	Maximum of spectral power density of normalized centered instantaneous amplitude, standard deviation of the absolute value of the centered non-linear component of instantaneous phase, standard deviation of centered non-linear component of direct instantaneous phase, standard deviation of absolute value of normalized centered instantaneous amplitude, kurtosis of the normalized instantaneous amplitude	[60]
F_8	Logscale power of delta (1-4HZ), theta (4-8HZ), and alpha (8-13HZ) bands	[41]
F_9	Mean amplitude of high frequency signals, slope of PSD curves between high and low frequencies, variance of inter-peak distance	[33]

(generalized) accuracy. Apart from FakeCatcher, we believe the second main contribution of this paper is to understand deep fakes in the wild. To our knowledge, generative models are not explored by biological signals before, and we present the first experimental literature survey for understanding and explaining human signals in synthetic portrait videos (Appendix A). We expect the observations discussed in Section 5.2 to enlighten future analysis of both generative noise and of deep fake detectors. We also encourage this line of research to continue by sharing our Deep Fakes dataset.

References

- [1] Ai art at christie's sells for \$432,500. <https://www.nytimes.com/2018/10/25/arts/design/ai-art-sold-christies.html>. Accessed: 2018-11-15. 1
- [2] Deep fakes: A looming crisis for national security, democracy and privacy? <https://www.lawfareblog.com/deep-fakes-looming-crisis-national-security-democracy-and-privacy>. Accessed: 2018-11-15. 1
- [3] Fake celebrity porn is blowing up on reddit, thanks to artificial intelligence. <https://www.theverge.com/2018/1/24/16929148/fake-celebrity-porn-ai-deepfake-face-swapping-artificial-intelligence-reddit>. Accessed: 2018-11-15. 1
- [4] D. Afchar, V. Nozick, J. Yamagishi, and I. Echizen. Mesonet: a compact facial video forgery detection network, 2018. 3, 7
- [5] AKTHI, Umar, RUL, RAKASH, ONRAD, S. T.T., and Ucker. Bounded kalman filter method for motion-robust , non-contact heart rate estimation. 2018. 3
- [6] B. Amos, B. Ludwiczuk, and M. Satyanarayanan. Openface: A general-purpose face recognition library with mobile applications. Technical report, CMU-CS-16-118, CMU School of Computer Science, 2016. 6
- [7] G. Balakrishnan, F. Durand, and J. Guttag. Detecting pulse from head motions in video. In *2013 IEEE Conference on Computer Vision and Pattern Recognition*, pages 3430–3437, June 2013. 3
- [8] J. Bao, D. Chen, F. Wen, H. Li, and G. Hua. Towards open-set identity preserving face synthesis. In *The IEEE Conference on Computer Vision and Pattern Recognition (CVPR)*, June 2018. 3
- [9] M. Barni, L. Bondi, N. Bonettini, P. Bestagini, A. Costanzo, M. Maggini, B. Tondi, and S. Tubaro. Aligned and non-aligned double jpeg detection using convolutional neural networks. *J. Vis. Comun. Image Represent.*, 49(C):153–163, Nov. 2017. 3
- [10] Z. Boulkenafet, J. Komulainen, and A. Hadid. Face spoofing detection using colour texture analysis. *IEEE Transactions on Information Forensics and Security*, 11(8):1818–1830, Aug 2016. 3
- [11] A. Brock, T. Lim, J. M. Ritchie, and N. Weston. Neural photo editing with introspective adversarial networks. *CoRR*, abs/1609.07093, 2016. 3

- [12] J. Buckheit, J. B. Buckheit, D. L. Donoho, and D. L. Donoho. Wavelab and reproducible research. pages 55–81. Springer-Verlag, 1995. 6
- [13] S. Butterworth. On the theory of filter amplifiers. 1930. 7
- [14] C.-C. Chang and C.-J. Lin. Libsvm: A library for support vector machines. *ACM Trans. Intell. Syst. Technol.*, 2(3):27:1–27:27, May 2011. 6
- [15] W. Chen and D. McDuff. Deepphys: Video-based physiological measurement using convolutional attention networks. In *The European Conference on Computer Vision (ECCV)*, September 2018. 3
- [16] Y. Choi, M. Choi, M. Kim, J.-W. Ha, S. Kim, and J. Choo. Stargan: Unified generative adversarial networks for multi-domain image-to-image translation. In *The IEEE Conference on Computer Vision and Pattern Recognition (CVPR)*, June 2018. 3
- [17] C. Cortes and V. Vapnik. Support-vector networks. *Machine Learning*, 20(3):273–297, Sep 1995. 5
- [18] G. de Haan and V. Jeanne. Robust pulse rate from chrominance-based rppg. *IEEE Transactions on Biomedical Engineering*, 60(10):2878–2886, Oct 2013. 3, 4, 7
- [19] H. Ding, K. Sricharan, and R. Chellappa. Exprgan: Facial expression editing with controllable expression intensity. *AAAI*, 2018. 3
- [20] L. Feng, L. Po, X. Xu, Y. Li, and R. Ma. Motion-resistant remote imaging photoplethysmography based on the optical properties of skin. *IEEE Transactions on Circuits and Systems for Video Technology*, 25(5):879–891, May 2015. 3, 4
- [21] J. Galbally and S. Marcel. Face anti-spoofing based on general image quality assessment. In *2014 22nd International Conference on Pattern Recognition*, pages 1173–1178, Aug 2014. 3
- [22] I. Goodfellow, J. Pouget-Abadie, M. Mirza, B. Xu, D. Warde-Farley, S. Ozair, A. Courville, and Y. Bengio. Generative adversarial nets. In Z. Ghahramani, M. Welling, C. Cortes, N. D. Lawrence, and K. Q. Weinberger, editors, *Advances in Neural Information Processing Systems 27*, pages 2672–2680. Curran Associates, Inc., 2014. 1, 2
- [23] I. Gulrajani, F. Ahmed, M. Arjovsky, V. Dumoulin, and A. C. Courville. Improved training of wasserstein gans. In I. Guyon, U. V. Luxburg, S. Bengio, H. Wallach, R. Fergus, S. Vishwanathan, and R. Garnett, editors, *Advances in Neural Information Processing Systems 30*, pages 5767–5777. Curran Associates, Inc., 2017. 3
- [24] Z. He, W. Zuo, M. Kan, S. Shan, and X. Chen. Arbitrary facial attribute editing: Only change what you want. *arXiv preprint arXiv:1711.10678*, 2017. 3
- [25] H. Hu, Y. Wang, and J. Song. Signal classification based on spectral correlation analysis and svm in cognitive radio. In *22nd International Conference on Advanced Information Networking and Applications (aina 2008)*, pages 883–887, March 2008. 5, 8
- [26] R. Huang, S. Zhang, T. Li, and R. He. Beyond face rotation: Global and local perception gan for photorealistic and identity preserving frontal view synthesis. In *The IEEE International Conference on Computer Vision (ICCV)*, Oct 2017. 3
- [27] S. Iizuka, E. Simo-Serra, and H. Ishikawa. Globally and Locally Consistent Image Completion. *ACM Transactions on Graphics (Proc. of SIGGRAPH 2017)*, 36(4):107:1–107:14, 2017. 2
- [28] N. Jatupaiboon, S. Pan-Ngum, and P. Israsena. Real-time eeg-based happiness detection system. In *TheScientificWorldJournal*, 2013. 5, 8
- [29] A. Kampouraki, G. Manis, and C. Nikou. Heartbeat time series classification with support vector machines. *IEEE Transactions on Information Technology in Biomedicine*, 13(4):512–518, July 2009. 8
- [30] T. Karras, T. Aila, S. Laine, and J. Lehtinen. Progressive growing of GANs for improved quality, stability, and variation. In *Proc. International Conference on Learning Representations (ICLR)*, 2018. 3
- [31] H. Kim, P. Garrido, A. Tewari, W. Xu, J. Thies, M. Niessner, P. Pérez, C. Richardt, M. Zollhöfer, and C. Theobalt. Deep video portraits. *ACM Trans. Graph.*, 37(4):163:1–163:14, July 2018. 3
- [32] D. P. Kingma, T. Salimans, R. Jozefowicz, X. Chen, I. Sutskever, and M. Welling. Improving variational inference with inverse autoregressive flow, 2016. 3
- [33] G. Koren. Wearable sensor for physiological data acquisition in early education. <https://github.com/get/PPG-Heart-Rate-Classifer/blob/master/thesis%20excerpt.pdf>, 2016. Accessed: 2018-11-15. 8
- [34] V. Kushwaha, M. Singh, R. Singh, M. Vatsa, N. Ratha, and R. Chellappa. Disguised faces in the wild. In *The IEEE Conference on Computer Vision and Pattern Recognition (CVPR) Workshops*, June 2018. 3, 5
- [35] H. Li, B. Li, S. Tan, and J. Huang. Detection of deep network generated images using disparities in color components, 2018. 3
- [36] Y. Li, M.-C. Chang, and S. Lyu. In ictu oculi: Exposing ai generated fake face videos by detecting eye blinking, 2018. 3, 7
- [37] Y. Li, S. Liu, J. Yang, and M.-H. Yang. Generative face completion. In *IEEE Conference on Computer Vision and Pattern Recognition*, 2017. 1, 3
- [38] X. Mao, Q. Li, H. Xie, R. Y. Lau, Z. Wang, and S. Paul Smolley. Least squares generative adversarial networks. In *The IEEE International Conference on Computer Vision (ICCV)*, Oct 2017. 3
- [39] A. S. M. Murugavel, S. Ramakrishnan, K. Balasamy, and T. Gopalakrishnan. Lyapunov features based eeg signal classification by multi-class svm. In *2011 World Congress on Information and Communication Technologies*, pages 197–201, Dec 2011. 5, 8
- [40] K. Nagano, J. Seo, J. Xing, L. Wei, Z. Li, S. Saito, A. Agarwal, J. Fursund, and H. Li. pagan: Real-time avatars using dynamic textures. *ACM Transactions on Graphics*, 2018. 1
- [41] D. Nie, X. Wang, L. Shi, and B. Lu. Eeg-based emotion recognition during watching movies. In *2011 5th International IEEE/EMBS Conference on Neural Engineering*, pages 667–670, April 2011. 5, 8

- [42] S. Pei and J. Ding. Relations between gabor transforms and fractional fourier transforms and their applications for signal processing. *IEEE Transactions on Signal Processing*, 55(10):4839–4850, Oct 2007. 5
- [43] M.-Z. Poh, D. J. McDuff, and R. W. Picard. Non-contact, automated cardiac pulse measurements using video imaging and blind source separation. *Opt. Express*, 18(10):10762–10774, May 2010. 3
- [44] A. Pumarola, A. Agudo, A. Martinez, A. Sanfeliu, and F. Moreno-Noguer. Ganimation: Anatomically-aware facial animation from a single image. In *Proceedings of the European Conference on Computer Vision (ECCV)*, 2018. 1
- [45] A. Radford, L. Metz, and S. Chintala. Unsupervised representation learning with deep convolutional generative adversarial networks, 2015. 1, 3
- [46] A. Rössler, D. Cozzolino, L. Verdoliva, C. Riess, J. Thies, and M. Nießner. Faceforensics: A large-scale video dataset for forgery detection in human faces. *arXiv*, 2018. 1, 2, 4, 5, 6, 7
- [47] P. V. Rouast, M. T. P. Adam, R. Chiong, D. Cornforth, and E. Lux. Remote heart rate measurement using low-cost rgb face video: a technical literature review. *Frontiers of Computer Science*, 12(5):858–872, Oct 2018. 3
- [48] A. Roy, D. Bhalang Tariang, R. Subhra Chakraborty, and R. Naskar. Discrete cosine transform residual feature based filtering forgery and splicing detection in jpeg images. In *The IEEE Conference on Computer Vision and Pattern Recognition (CVPR) Workshops*, June 2018. 3
- [49] W. Shen and R. Liu. Learning residual images for face attribute manipulation. *2017 IEEE Conference on Computer Vision and Pattern Recognition (CVPR)*, pages 1225–1233, 2017. 3
- [50] M. Soleymani, J. Lichtenauer, T. Pun, and M. Pantic. A multimodal database for affect recognition and implicit tagging. *IEEE Trans. Affect. Comput.*, 3(1):42–55, Jan. 2012. 5, 8
- [51] S. Tariq, S. Lee, H. Kim, Y. Shin, and S. S. Woo. Detecting both machine and human created fake face images in the wild. In *Proceedings of the 2Nd International Workshop on Multimedia Privacy and Security*, MPS ’18, pages 81–87, New York, NY, USA, 2018. ACM. 3
- [52] A. Tewari, M. Zollhofer, H. Kim, P. Garrido, F. Bernard, P. Perez, and C. Theobalt. Mofa: Model-based deep convolutional face autoencoder for unsupervised monocular reconstruction. In *The IEEE International Conference on Computer Vision (ICCV)*, Oct 2017. 3
- [53] J. Thies, M. Zollhöfer, M. Stamminger, C. Theobalt, and M. Nießner. Face2Face: Real-time Face Capture and Reenactment of RGB Videos. In *Proc. Computer Vision and Pattern Recognition (CVPR)*, IEEE, 2016. 3, 7
- [54] S. Tulyakov, X. Alameda-Pineda, E. Ricci, L. Yin, J. F. Cohn, and N. Sebe. Self-adaptive matrix completion for heart rate estimation from face videos under realistic conditions. In *The IEEE Conference on Computer Vision and Pattern Recognition (CVPR)*, June 2016. 3, 4
- [55] P. Viola and M. J. Jones. Robust real-time face detection. *Int. J. Comput. Vision*, 57(2):137–154, May 2004. 3
- [56] T.-C. Wang, M.-Y. Liu, J.-Y. Zhu, G. Liu, A. Tao, J. Kautz, and B. Catanzaro. Video-to-video synthesis. In *Advances in Neural Information Processing Systems (NIPS)*, 2018. 1, 3
- [57] P. Welch. The use of fast fourier transform for the estimation of power spectra: A method based on time averaging over short, modified periodograms. *IEEE Transactions on Audio and Electroacoustics*, 15(2):70–73, June 1967. 7
- [58] H.-Y. Wu, M. Rubinstein, E. Shih, J. Guttag, F. Durand, and W. Freeman. Eulerian video magnification for revealing subtle changes in the world. *ACM Trans. Graph.*, 31(4):65:1–65:8, July 2012. 3
- [59] R. Xu, Z. Zhou, W. Zhang, and Y. Yu. Face transfer with generative adversarial network. *CoRR*, abs/1710.06090, 2017. 3
- [60] W. Zhang. Automatic modulation classification based on statistical features and support vector machine. In *2014 XXXIth URSI General Assembly and Scientific Symposium (URSI GASS)*, pages 1–4, Aug 2014. 5, 8
- [61] C. Zhao, C.-L. Lin, W. Chen, and Z. Li. A novel framework for remote photoplethysmography pulse extraction on compressed videos. In *The IEEE Conference on Computer Vision and Pattern Recognition (CVPR) Workshops*, June 2018. 3, 7
- [62] J.-Y. Zhu, T. Park, P. Isola, and A. A. Efros. Unpaired image-to-image translation using cycle-consistent adversarial networks. In *Computer Vision (ICCV), 2017 IEEE International Conference on*, 2017. 1, 3